



## Structural stability of biofilms produced from silkworm cocoon fibers

ANA LÚCIA DE SOUZA MADUREIRA FELÍCIO and HENRIQUE DE SANTANA\*

Departamento de Química, CCE, Universidade Estadual de Londrina, Londrina,  
PR 86051-990, Brazil

(Received 11 June, revised 21 July, accepted 23 July 2021)

**Abstract:** Biofilms were obtained from cocoons of the silkworm, *Bombyx mori*, involving the removal of sericin, extraction and solubilization of fibroin fibers, dialysis of fibroin dispersions and preparation of biofilms by the casting process. Biofilm transparency was verified by UV–Vis spectroscopy and thermal stability by thermogravimetric/differential scanning calorimetry (TG/DSC). Soon after preparation, the solidification of the fibroin solution prepared from the cocoons and extracted by the Ajisawa method was monitored until the biofilm stabilized, using attenuated total reflectance-Fourier transform infrared spectroscopy (ATR-FTIR) as a function of time. The results showed that there was a change in the conformation from the silk I structure ( $\alpha$ -helix) to silk II ( $\beta$ -sheet). In order to improve the characterization of the biofilms obtained by the Ajisawa method and LiBr solubilization of fibroin fibers, Raman spectroscopy was used to verify the stabilization of the different possible molecular conformations for the fibers in these materials, by comparison with the cocoon spectra and those of the solid (freeze-dried precipitated by dialysis for 72 h. By comparing the Raman spectra of the biofilms in terms of the intensities of the broadened band characteristic of amide I, it was possible to assess the conformational changes in both materials based on the possible transitions between  $\beta$ -sheet conformations and flexible  $\alpha$ -helix and  $\beta$ -turn structures. The results showed a dispersion of these conformations in the biofilms generated and in the solid freeze-dried hydrogel spectrum, and the  $\beta$ -sheet conformation was found to be predominant. The TG and DSC curves showed that the materials with higher  $\beta$ -sheet content exhibited higher thermal stability. Thus, the data obtained further elucidated the properties of these materials that are widely used in various processes.

**Keywords:** silk fibroin; Raman spectroscopy; *Bombyx mori*; molecular conformation.

\*Corresponding author. E-mail: hensan@uel.br  
<https://doi.org/10.2298/JSC210611054F>

## INTRODUCTION

The search for sustainable materials with applications in various fields has become the focal point of various studies in pursuit of process innovation. One such material is the fiber produced and synthesized in the glands of the silkworm, *Bombyx mori*.<sup>1–18</sup> At the end of the larval stage, the silkworm produces silk fibers to form a cocoon by a complex spinning process. Most of the cocoon consists of fibroin fibers cemented together by another protein, sericin, that acts as an adhesive.<sup>1</sup>

The sericin is removed by degumming the cocoon, and the silk fibroin (SF) can be processed using various methods. Conventional degumming entails boiling the cocoons in an aqueous solution, the efficiency of which can be improved by adding substances such as sodium carbonate, high lipid soaps, citric acid, urea, tartaric acid or various enzymes to remove the sericin and other impurities.<sup>2</sup>

After degumming, the fibroin fibers can be dissolved in various concentrated salt solutions, such as lithium bromide (LiBr), calcium chloride (CaCl<sub>2</sub>), calcium nitrate Ca(NO<sub>3</sub>)<sub>2</sub>, Ajisawa reagent (CaCl<sub>2</sub>:EtOH:H<sub>2</sub>O) and formic acid. The salt concentration, temperature and dissolution time can directly affect the degree of peptide bond decomposition and consequently the solubility of the fibroin. The salts involved in both degumming and dissolution are removed by dialysis to obtain an aqueous SF solution.<sup>1,3–5</sup>

The aqueous SF solution can be used as is or to produce versatile forms of fibroin, such as powder, nanofibers, films, hydrogels and sponges, according to the field of application, and by virtue of its biocompatibility, controllable degradation, ease of processing and availability in the sericulture industry.<sup>3,6</sup>

SF biofilms are one of the most important and valuable support biomaterials with applications in fields such as biomedicine, electronics, textile engineering, optoelectronics, energy collection/storage, biosensors, food coatings, *etc.* They can be obtained by simple evaporation of the aqueous solution (a process known as casting), or by more complex techniques, such as vertical deposition, spin-assisted layer-by-layer assembly, spin coating or electrospinning.<sup>7</sup>

SF has two main molecular conformations (silk I and silk II) in the secondary structure. Silk I is a non-crystalline, metastable, water soluble form and is mainly made up of random coils and  $\alpha$ -helix conformations. Silk II is a highly stable, organized, non-water-soluble structure, characterized by a sheet formation. The structures can be transformed under appropriate conditions. The molecular conformation of the SF is an important parameter in the production of medical devices.<sup>8–11</sup>

In fact, native SF can be solubilized and processed as regenerated silk in a wide variety of geometrical shapes. Several studies have shown that chemical treatments, such as immersion in high salt concentration organic solvents, can break the hydrogen bond between the  $\beta$ -sheets to transition the SF conformation

from silk II to silk I and transform fibroin fibers into a water-soluble random coil conformation.<sup>19,20</sup>

Motta *et al.*<sup>21</sup> report on the thermal and dynamic mechanical properties of three different regenerated silk fibroin films cast from water solutions, characterized by differential scanning calorimetry (DSC). DSC revealed the presence of a lower temperature endothermic phenomenon centered at about 70 °C for the as-prepared room temperature cast film, and other typical material thermal parameters – glass transition, crystallization, and thermal degradation – more or less pronounced depending on the specific preparation procedure and the thermal or solvent treatment. These results were interpreted assuming progressive evolution of the random coil regions from the more stable  $\beta$ -sheet conformation, as induced by different applied preparation conditions or treatment.

The aim of this study was to examine the structural organization and thermal stability of biofilms with a view to elucidating the properties of this material. Attenuated total reflectance-Fourier transform infrared (ATR-FTIR) and Raman spectroscopy were used to characterize the segment arrangements in the polypeptide matrices for generation to produce biofilms, and thermogravimetric (TG) and differential scanning calorimetry (DSC) to monitor the effect of temperature on the various materials. The results show that the  $\beta$ -sheet conformation plays a crucial role in the so-called secondary fibroin structures of biofilms, determining the rigidity and thermal stability of the material.

## EXPERIMENTAL

### Materials

The silkworm cocoons (*Bombyx mori*) used in this study were imported from China. Fibers were extracted and solubilized using anhydrous Na<sub>2</sub>CO<sub>3</sub> (Sigma-Aldrich, 99.0 %), ultrapure water (Milli-Q, Milipore), CaCl<sub>2</sub>·2H<sub>2</sub>O (Dinâmica, 99 %) and ethanol (Qhemis, 99.5 %).

### Cocoon classification

First, the cocoon samples were cut along the top to remove the pupae and other internal impurities. Then they were cut into small pieces of approximately 1 cm<sup>2</sup> and washed in ultrapure water.

### Fibroin extraction – sericin removal (degumming)

A quantity of 1.06 g Na<sub>2</sub>CO<sub>3</sub> was dissolved in a beaker containing 500 mL of ultrapure water heated to 95 °C on a hotplate. Next, 1.5 g of chopped cocoons were added. The apparatus was constantly stirred and kept at 95 °C for 40 min.

After heating and stirring, the fibers were taken out of the solution and excess water removed by manual wringing. The fibers were then washed in ultrapure water at 25 °C and stirred for 20 min. The washing was repeated 3 times and the excess water then removed by manual wringing. The resulting fibers were placed in a Petri dish and left in an oven at 50 °C for 24 h.

This degumming stage resulted in an average drop in the initial cocoon weight of 27.6 %, representing the amount of sericin removed during the process.

*Solubilization of the fibroin fibers*

Fiber solubilization can be achieved by different methods using different salts and solvents. In this study, two fiber solubilization methods were used.

First, a ternary solution (Ajisawa reagent) consisting of calcium chloride, ethanol and water ( $\text{CaCl}_2 \cdot 2\text{H}_2\text{O} : \text{CH}_3\text{CH}_2\text{OH} : \text{H}_2\text{O}$ , 1:2:6 mole ratio) was prepared. The fibers obtained in the previous stage were cut into smaller pieces and added to the solution at 1 g of chopped fiber to 10 mL ternary solution (1:10).

The beaker containing the solution was then placed in a thermostat-controlled bath at 80 °C for 40 min, stirring manually every 5 min. The beaker was then removed from the bath and left to cool to a temperature of 25 °C. The fibers were completely solubilized in the ternary solution, resulting in low-viscosity, slightly bleached dispersions.

In the second method, a 9.3 mol L<sup>-1</sup> aqueous solution of lithium bromide (LiBr) was prepared. Care is required in the preparation of this solution, since the reaction produces a lot of heat. The dry fibers were also cut into smaller pieces and added to the solution at 1 g of fiber to 4 mL solution (1:4).

The solution was then placed in a thermostat-controlled bath at 60 °C for approximately 4 h, stirring manually every 5 min for the first hour, and then every 15 min until the fibers were fully dissolved. Next, the beaker was removed from the bath and left to cool to 25 °C, as in the Ajisawa method, whereby a similar dispersion was obtained.

*Dialysis*

The fibroin dispersions obtained using the two methods were transferred to pre-hydrated cellulose membranes, then dialyzed in ultrapure water for 48 h. The temperature was kept at 25 °C with continuous stirring, and the initial water was replaced after 1 h, and subsequently every 8 h, at 1:30 volume ratio fibroin dispersion:water.

After dialysis, the dispersion was transferred to 50 mL Falcon tubes for centrifugation at 6000 rpm (Centurion Pro-Analytical centrifuge) for 40 min to remove impurities. The supernatant was transferred to another tube and the process repeated.

The dispersions dialyzed for 24 h were transparent and colorless, and the bleached particles precipitated by centrifugation adhered to the wall and bottom of the tube. The supernatant of the dispersion was collected and transferred to another tube, completely eliminating these particles. The fibroin solution was stored at 4 °C before use.

A volume of 0.5 mL of each dispersion was placed in weighing boats and kept in an oven at 60 °C for 24 h. The weight after drying was checked by calculating the weight/volume of dialyzed cocoon fibroin, resulting in an average of 5.0 %.

To check whether the dialysis time influenced purification, another part of the fiber dispersion was left to dialysis for a further 24 h, totaling 72 h. In this case, it formed a hydrogel precipitate on the inside of the membrane. This material was removed, centrifuged under the conditions applied to the 48 h dispersion, and subsequently freeze-dried to remove the water, leaving a solid residue.

*Biofilm preparation*

Biofilms were prepared by casting the fibroin solution dialyzed for 48 h. A volume of 0.8 mL fibroin solution was transferred to 23 mm acrylic plates, placed in a fan oven and kept at 50 °C for 8 h. Next, the films were carefully removed using tweezers and characterized.

After drying, the biofilms were transparent and looked like plastic. There was some flexibility and no breaks were observed.

### Spectroscopic characterization

To check the transparency of the as prepared biofilms, UV–Vis transmittance spectra in the 220–800 nm range were obtained using a UV–Vis 2600 spectrophotometer (Shimadzu).

Infrared spectra were taken on a Fourier transform IR spectrophotometer (FTIR, Frontier MIR/NIR, PerkinElmer®) in the attenuated total reflectance (ATR) mode, using a UATR® accessory with diamond crystal and zinc selenide focusing, scan between 4000 and 650 cm<sup>-1</sup>, resolution of 2 cm<sup>-1</sup> and 32 accumulated scans. The biofilm was formed over the crystal, and the spectra acquired over a period of 60 min in a gaseous nitrogen atmosphere to speed up the drying process.

Raman spectra were obtained using an Alpha300+ WITec® confocal Raman microscope system (excitation at 785 nm), with a ZEISS 50× lens.

### Thermal analysis

Biofilm fragments with a total weight of 1.8 g were used in differential scanning calorimetry (DSC) and thermogravimetric (TG) analysis. Samples were placed on hermetically sealed aluminum (DSC) and platinum (TG) supports. The DSC curves were obtained using a Shimadzu DSC-60, and the heating rate was 10 °C min<sup>-1</sup> in the 230–300 °C range. TG curves were obtained using a Shimadzu TGA-50 and the heating rate was 10 °C min<sup>-1</sup> in the 20–1000 °C range. The gas flow for both procedures was 50 mL min<sup>-1</sup> nitrogen.

## RESULTS AND DISCUSSION

The UV–Vis spectra of the biofilms obtained by the two extraction methods, a) Ajisawa and b) LiBr, are shown in Fig. S-1 of the Supplementary material to this paper. High incidences of transparency in the visible region (300–800 nm) and a characteristic band at 277 nm were observed for both analyzed biofilms. This peak could be ascribed to the  $\pi\rightarrow\pi^*$  electron transition of aromatic, tyrosine, phenylalanine and tryptophan amino acid residues in the fibroin chain.<sup>4,9</sup>

The elevated transparency of the biofilms was a desired characteristic given the various possible applications of this kind of material, whether in optics or even biomedical fields (encapsulating drugs, colorants, nanoparticles, *etc.*). Some studies in the literature show that transparency can be directly associated with the method used to obtain the fibroin solution. Biofilms obtained using regenerated fibroin from cocoons exhibit transparency indices above 95 %, whereas for biofilms from native fibroin extracted directly from the silkworm glands, this index was between 70 and 90 %, and in addition to opacity, the films may exhibit yellowish hues.<sup>20</sup>

The ATR FT-IR spectra as a function of the structural stabilization time of the biofilm prepared by Ajisawa extraction are shown in Fig. 1. Initially (up to 4 min after preparation) low intensity bands were observed at 1643, 1546 and 1246 cm<sup>-1</sup>, attributed respectively to amides I, II and III.<sup>5</sup> Amide I is the result of asymmetric coupling of C=O and C–N bond stretching, and the band related to amides II and III are the result of symmetric coupling of C–N bond stretching and angular deformation in the N–H plane.<sup>10</sup> All these bands in the IR spectrum are sensitive to changes in the conformation.<sup>11</sup>

After 45 min, an increase in the intensity of these bands was observed, with broadened bands between 1650/1639, 1531/1514 and 1240/1231  $\text{cm}^{-1}$ . After 60–65 min, the spectra remained unchanged. Bands were defined at 1639, 1514 and 1231  $\text{cm}^{-1}$  and shoulders were observed at 1650 and 1531  $\text{cm}^{-1}$ .

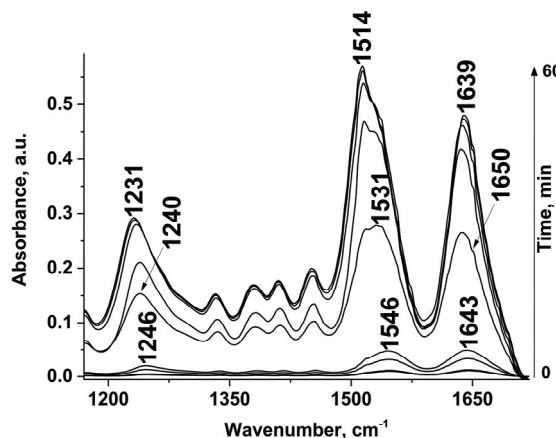


Fig. 1. Changes in the FTIR spectra as a function of the structural stabilization time of the biofilm prepared by the Ajisawa extraction method, obtained by ATR.

According to the literature,<sup>11</sup> the bands at 1610–1630  $\text{cm}^{-1}$  (amide I) and 1510–1520  $\text{cm}^{-1}$  (amide II) are characteristic of silk II ( $\beta$ -pleated sheet) secondary structure, whereas absorption at 1640–1660  $\text{cm}^{-1}$  (amide I) and 1535–1542  $\text{cm}^{-1}$  indicate that the conformation contains silk I ( $\alpha$ -form). These results could indicate that after 60–65 min, a biofilm stabilized with a predominance of the  $\beta$ -sheet rather than the  $\alpha$ -form.<sup>11,12</sup>

With the aim of further investigating the changes observed in the IR spectra, Raman spectra were recorded. This was necessary in view of the work performed by Lefèvre *et al.*<sup>13</sup> who used polarized Raman spectroscopy to show the molecular organization in the silk cocoon produced by *B. mori*, with a mixture of different quantities of  $\beta$ -sheets and flexible structures ( $\beta$ -turns and  $\alpha$ -helices).

The Raman spectra of the cocoon, the biofilms prepared by the LiBr and Ajisawa methods, and the freeze-dried hydrogel are shown in Fig. 2.

The Raman spectra of the cocoon (Fig. 2), obtained at an excitation wavelength of 785 nm, exhibit main bands at around 1672, 1622, 1560, 1455, 1407, 1270 and 1239  $\text{cm}^{-1}$ .<sup>14</sup> The frequencies at 1672, 1560 and 1270/1239  $\text{cm}^{-1}$  were respectively ascribed to amides I, II and III, related to the different contributions of C=O stretching, angular N–H in-plane deformation and C–N stretching in the polypeptide chains of the cocoon primary structure. The band at 1622  $\text{cm}^{-1}$  was related to vibrations in the amino acid side-chain of the silk fibroin. The band at 1407  $\text{cm}^{-1}$  was related to the presence of sericin, and the band at 1455  $\text{cm}^{-1}$  was ascribed to fibroin.<sup>15,18</sup>

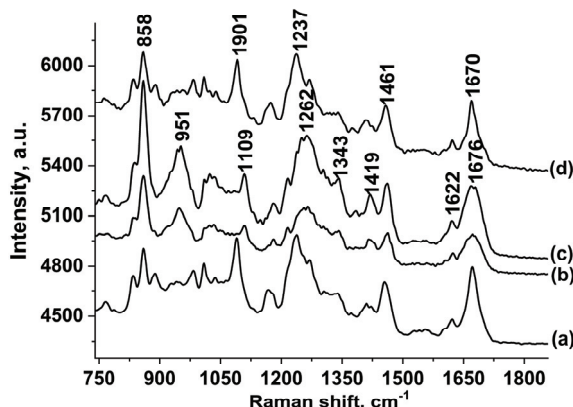


Fig. 2. Raman spectra of: a) cocoon, b) biofilms prepared by the LiBr method and c) Ajisawa method, and d) the freeze-dried hydrogel, at excitation of 785 nm.

The biofilm spectra exhibited marked variations compared to the spectrum of the cocoon sample. The spectra in Fig. 2b and c show band displacement and broadening compared to the cocoon spectra at 1674, 1461 and 1419 cm<sup>-1</sup>, as well as the presence of a broadened band at 1262 cm<sup>-1</sup>. These spectral variations were considered to be associated with structural changes in the material. The spectrum of the freeze-dried hydrogel (Fig. 2d), was fairly similar to that obtained for the cocoon, exhibiting preferential ordering of the materials that was different from that observed in the spectra of the biofilms.

To better assess whether the biofilms prepared were or were not identical at molecular level, the work of Lefèvre *et al.*<sup>13</sup> was taken into account. The deconvolution of the amide I band in the Raman spectrum revealed that the frequencies at 1655, 1666 and 1678/1693 cm<sup>-1</sup> could be related to different conformations of the  $\alpha$ -helix,  $\beta$ -sheet and  $\beta$ -turn structures, respectively.

With the aim of studying the Raman spectra of the biofilms, deconvolution was implemented in the spectra between 1620/1640 and 1700/1710 cm<sup>-1</sup>, as shown in Fig. 3. Fig. 3 shows the four bands in the spectra analyzed, compared to the different conformations proposed by Lefèvre *et al.*<sup>13</sup> The cocoon spectrum (Fig. 3a) shows that the band at 1671 cm<sup>-1</sup> was of higher intensity and broader compared to the bands at 1652 and 1687 cm<sup>-1</sup>, revealing that the cocoon structure has a tendency to incorporate a higher quantity of  $\beta$ -sheet conformations. However, the deconvoluted spectrum of the biofilm produced by extraction with LiBr (Fig. 3b), that there were more  $\alpha$ -helices and  $\beta$ -turns than  $\beta$ -sheets because of the higher relative intensity and broadening of the bands at 1660 and 1679/1689 cm<sup>-1</sup>, compared to that at 1670 cm<sup>-1</sup>.

In the deconvoluted spectrum of the biofilm obtained by Ajisawa extraction (Fig. 3c), the results were predominantly intermediate between those obtained for

the cocoon and the biofilm extracted with LiBr. A higher intensity was observed for the band at  $1667\text{ cm}^{-1}$  and lower intensity of the bands at  $1652$  and  $1680\text{ cm}^{-1}$ , respectively related to the  $\alpha$ -helix and  $\beta$ -turn conformations, despite the fact that the band at  $1684\text{ cm}^{-1}$  was fairly broad and intense, impeding more accurate analysis.

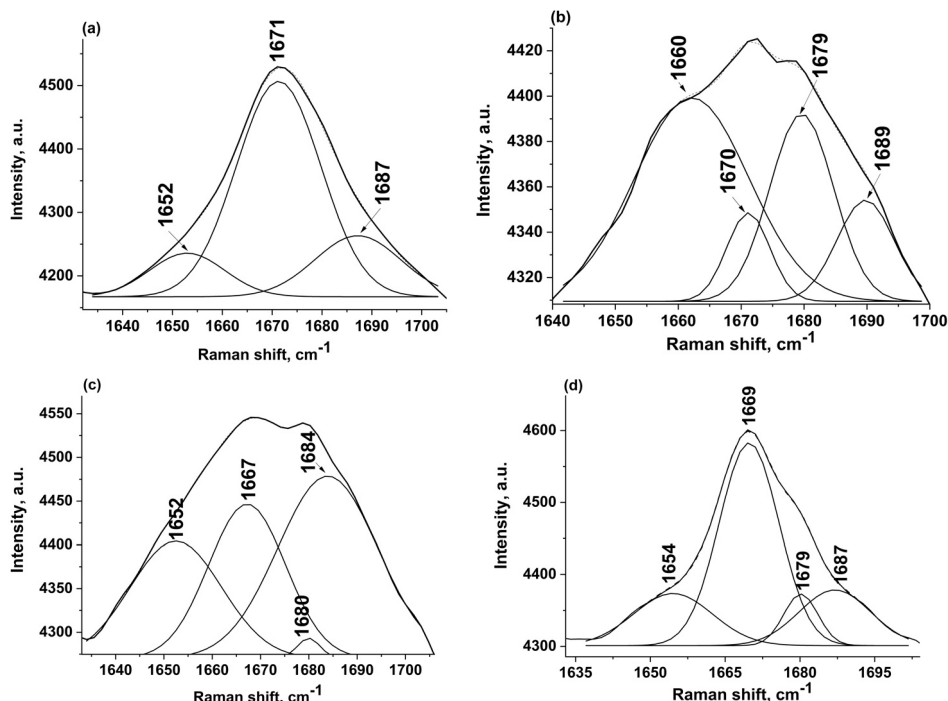


Fig. 3. Deconvoluted Raman spectra of: a) cocoon, biofilms prepared by: b) the LiBr method and c) the Ajisawa method, and d) the freeze-dried hydrogel.

These results show that the structural ordering of the biofilms is the opposite of that encountered in the cocoon, where there is a mixture of  $\beta$ -sheet,  $\alpha$ -helix and  $\beta$ -turn conformations, exhibiting greater malleability and stability.

Similar results were obtained in other studies, in which biofilms produced by Ajisawa extraction contained slightly more  $\beta$ -sheets and less  $\beta$ -turns than those produced by solubilization with LiBr.<sup>20</sup> Defining the conformation of biofilms is particularly important and advantageous, depending on the applications envisaged. The conformation of the material can significantly influence characteristics such as biodegradation, mechanical and optical properties, and even biological compatibility conditions. For instance, a biofilm with a predominance of  $\beta$ -turns and  $\alpha$ -helices would be highly soluble in water and more biodegradable compared to a biofilm with a predominance of secondary structures, such as  $\beta$ -sheets, but this material would be more flexible and mechanically stronger than the other.<sup>20</sup>

It was observed that the dialysis time and conditions precipitated a rigid solid originating from the gel prepared from the cocoons. Based on the previous characterization of the biofilm Raman spectra, the same spectrum deconvolution procedures were performed for the freeze-dried hydrogel in the 1624–1710 cm<sup>-1</sup> range, as shown in Fig. 3d.

The deconvoluted spectrum showed narrower bands than those previously observed in the cocoon and biofilm deconvoluted spectra (Fig. 3a–c). Regarding the spectrum of the solid originating from the cocoons (Fig. 3a), in the deconvoluted spectrum of the hydrogel (Fig. 3d), the relative intensities of the bands remained the same as those in the cocoon spectrum. The band at 1679 cm<sup>-1</sup> could be observed, due to the narrower bandwidth obtained by deconvolution.

Considering that the properties of the prepared biofilms can also be better verified by thermal analysis techniques, assuming that the thermal events developed with these techniques should promote a higher or lower degree of structural disorder in the molecular organization of the fibers that form the biomaterial, these materials were subjected to temperature variations and the modifications were monitored by the differential scanning calorimetry (DSC) and thermogravimetric (TG) techniques.

Sacco and de Santana<sup>14</sup> investigated the effect of temperature on the destabilization of the molecular conformation of silk fiber structures using confocal Raman spectroscopy and differential scanning calorimetry (DSC). The results indicated that, for the different cocoon samples, there was a drop in the  $\beta$ -sheet conformation compared to that of the  $\alpha$ -helix, and this structural disordering was caused by increased temperature. Similarly, a transition was observed in the conformation from  $\beta$ -sheet to  $\beta$ -turn as a result of the temperature applied.

The DSC curves in the 230–300 °C temperature range for the biofilms obtained by the two extraction methods are shown in Fig. S-2 of the Supplementary material. The biofilms were less stable to heat conditions than the silkworm cocoon. Sacco and de Santana<sup>14</sup> reported that at around 315 °C, the cocoon underwent an endothermal event, related to the thermal process associated with cocoon structure.

The biofilm prepared using LiBr (Fig. S-2a) exhibited an endothermal peak associated with a thermal event with a maximum of 274 °C, and for the Ajisawa biofilm at 280 °C (Fig. S-2b). Thus, the fact that the endothermal event occurred at a lower temperature for the LiBr biofilm compared to the Ajisawa biofilm must mean that the LiBr biofilm was less thermally stable due to the different aggregates present in these materials, due to stabilization of the different molecular conformations for the fibroin fibers as shown in the Raman results.

However, based on the work of Freddi *et al.*,<sup>22</sup> the thermal degradation of fibroin biofilm at temperatures lower than 290 °C is a characteristic of amorphous

phous biofilms (silk I), *i.e.*, biofilms that have not been subjected to any kind of physical or chemical treatment to alter the structure to a more crystalline form.

With the aim of better assessing the thermal behavior of these biofilms, thermogravimetric (TG) experiments were conducted.

The thermogravimetric curves for the cocoon, biofilms and freeze-dried hydrogel at temperatures between 20 and 1000 °C, verifying residual mass, and the differential residual mass curves for each material are shown in Fig. 4.

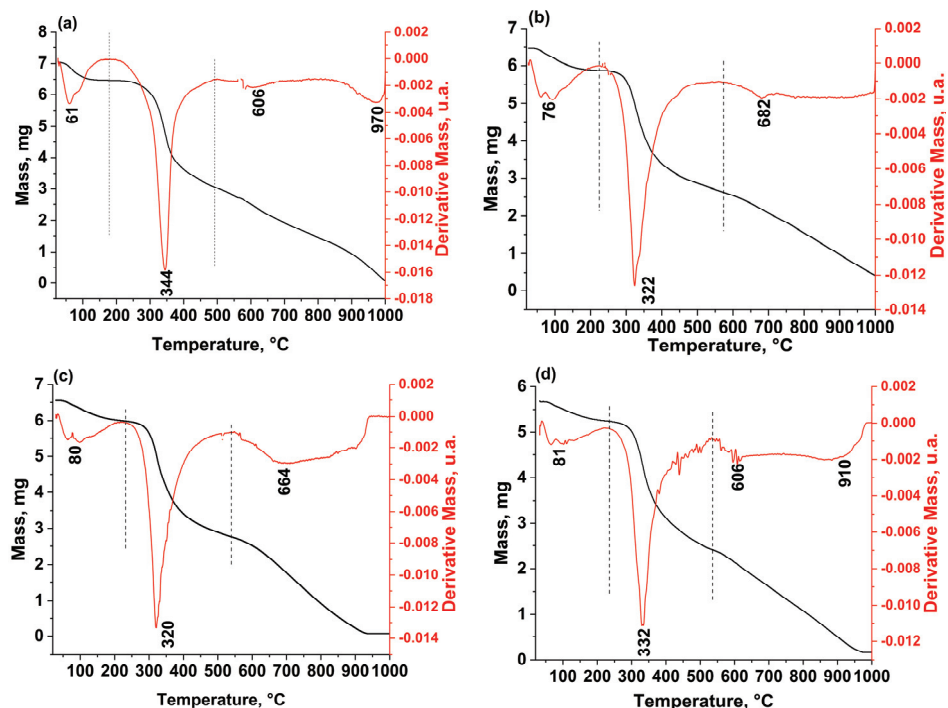


Fig. 4. Thermogravimetric curves of: a) cocoon, biofilms prepared by: b) the Ajisawa method and c) by the LiBr method, and d) the freeze-dried hydrogel.

Losses in mass of 8.1 % were observed for the cocoon (Fig. 4a), 9.4 % for the Ajisawa biofilm (Fig. 4b), 8.5 % for the LiBr biofilm (Fig. 4c) and 7.4 % for the freeze-dried hydrogel (Fig. 4d), at approximate respective maximum temperatures of 61, 76, 80 and 81 °C, which were attributed to water evaporation.

As the thermal process proceeded, different events were observed in the cocoon material, biofilms and the freeze-dried hydrogel. Around 43.5 % of the cocoon material underwent an initial decomposition process at an approximate maximum temperature of 344 °C (Fig. 4a). For the Ajisawa biofilm (Fig. 4b), the values were 40.5 % and 322 °C, and for the LiBr biofilm (Fig. 4c), 42.1 % and 320 °C. In other words, the main thermal degradation process for silk proteins

occurs because of the decomposition of the main structures of the protein molecular skeleton, showing the higher thermal stability of the cocoon material. The freeze-dried hydrogel produced intermediate results for this process, with a loss of 42.7 % at 332 °C (Fig. 4d).

However, another event was initiated close to a temperature of 492 °C, with maxima of 606 and 970 °C, decomposing 42.2 % of the cocoon structure (Fig. 4a). Similarly, at around 574 °C the Ajisawa biofilm (Fig. 4b) loses a further 33.2 % of its mass, whereas at 539 °C the LiBr biofilm (Fig. 4c) loses 41.3 %. This second event is probably attributable to carbonization. The freeze-dried hydrogel once again produced intermediate results, with a 39.7 % loss initiated at 533 °C (Fig. 4d). Residues of all materials were still observed, even at this temperature.

#### CONCLUSIONS

Using an adapted method from the literature for preparing biofilms by different processes, materials of high quality were prepared in terms of transparency and thermal stability.

Raman spectroscopy was found to be adequate for characterizing the structural ordering of the experimentally produced biofilms.

The results for the most rigid material, the freeze-dried hydrogel, showed a preference for the  $\beta$ -sheet conformation. Biofilms, which are more malleable, can show a tendency to produce a higher quantity of  $\alpha$ -helix and  $\beta$ -turn conformations. The two bands related to the  $\beta$ -turn conformation were absent only for the cocoon material, perhaps due to the rigidity of the bonds, as shown by its higher thermal stability.

Based on the thermal analysis and Raman results, it could be inferred that the biofilms with higher amounts of  $\beta$ -sheet conformations could be more thermally resistant.

The fibroin solubilization processes influenced the conformations and structural ordering, as revealed by the different techniques used in this study. The fiber solubilization method for obtaining the fibroin solution can be chosen based on what is most appropriate for the intended application of the material.

#### SUPPLEMENTARY MATERIAL

Additional data and information are available electronically at the pages of journal website: <https://www.shd-pub.org.rs/index.php/JSCS/article/view/10850>, or from the corresponding author on request.

*Acknowledgements.* We would like to express our appreciation to the Spectroscopy Laboratory (SPEC) at the PROPPG/UEL Multiuser Center. This study was funded under the Paraná State's SETI project (Silk, the transformative fiber). We would also like to thank the National Council for Scientific and Technological Development for its support.

И З В О Д  
СТРУКТУРНА СТАБИЛНОСТ БИОФИЛМОВА ДОБИЈЕНИХ ОД ВЛАКАНА ЧАУРА  
СВИЛЕНЕ БУБЕ

ANA LÚCIA DE SOUZA MADUREIRA FELÍCIO и HENRIQUE DE SANTANA

*Departamento de Química, CCE, Universidade Estadual de Londrina, Londrina, PR 86051-990, Brazil*

Биофилмови су добијени из чаура свилене бубе, *Bombyx mori*, уклањањем серицина, екстракцијом и солубилизацијом фибринских влакана, дијализом фибринских дисперзија и припремом биофилмова поступком ливења. Транспаренција биофилмова је верификована UV-видљивом спектроскопијом, а термална стабилност термогравиметријском/диференцијално сканирајућом калориметријском анализом (TG/DSC). Након припреме, очвршћивање фибринског раствора припремљеног из чаура и екстрахованог Ajisawa методом је праћено до стабилизације биофилма, применом ослабљене тоталне рефлексије (ATR-FTIR) у функцији времена. Резултати су показали да долази до конформационе промене из свила I ( $\alpha$ -хеликс) у свила II ( $\beta$ -раван) структуру. Да би се унапредила карактеризација биофилмова добијених Ajisawa методом и LiBr солубилизацијом фибринских влакана, коришћена је Раманска спектроскопија за верификацију стабилности различитих молекуларних конформација влакана у овим материјалима, поређењем спектра чауре и спектара талога (лиофилизовани хидрогел) преципитираних дијализом 72 сата. Поређењем Раманских спектара биофилмова и то интензитета проширене траке карактеристичне за амид I, могуће је добити информације о конформационим променама између  $\beta$ -равни и флексибилних структура  $\alpha$ -хеликса и  $\beta$ -завојнице. Резултати су показали дисперзију ових конформација у добијеним биофилмовима и у спектрима чврстих лиофилизованих хидрогелова, а конформација  $\beta$ -равни је преовлађујућа. TG и DSC криве су показале да материјал са већим садржајем  $\beta$ -равни показује већу термалну отпорност. Резултати добијени у овом раду доприносе бољем разумевању особина материјала који имају широку примену и бројним процесима.

(Примљено 11. јуна, ревидирано 21. јула, прихваћено 23. јула 2021)

#### REFERENCES

1. S. D. A. Cervantes, D. V. Cervantes, L. M. Olmo, J. L. Cenis, A. A. L. Pérez, *Mater. Sci. Eng., C* **33** (2013) 1945 (<https://dx.doi.org/10.1016/j.msec.2013.01.001>)
2. H. Yamada, H. Nakao, Y. Takasu, K. Tsubouchi, *Mater. Sci. Eng., C* **14** (2001) 41 ([https://dx.doi.org/10.1016/S0928-4931\(01\)00207-7](https://dx.doi.org/10.1016/S0928-4931(01)00207-7))
3. L. D. Koh, Y. Cheng, C. P. Teng, Y. W. Khin, X. J. Loh, S. Y. Tee, L. M. E. Ye, H. D. Yu, Y. W. Zhang, M. Y. Han, *Prog. Polym. Sci.* **46** (2015) 86 (<https://dx.doi.org/10.1016/j.progpolymsci.2015.02.001>)
4. W. I. Abdel-Fattah, N. Atwa, W. A. Ghareib, *Prog. Biomater.* **4** (2015) 77 (<https://dx.doi.org/10.1007/s40204-015-0039-x>)
5. X. Chen, Z. Shao, N. S. Marinkovic, L. M. Miller, P. Zhou, M. R. Chance, *Biophys. Chem.* **89** (2001) 25 ([https://dx.doi.org/10.1016/s0301-4622\(00\)00213-1](https://dx.doi.org/10.1016/s0301-4622(00)00213-1))
6. L. D. Koh, J. Yeo, Y. Y. Lee, Q. Ong, M. Han, B. C. K. Tee, *Mater. Sci. Eng., C* **86** (2018) 151 (<https://dx.doi.org/10.1016/j.msec.2018.01.007>)
7. Y. Qi, H. Wang, K. Wei, Y. Yang, R. Y. Zheng, I. S. Kim, K. Q. Zhang, *Int. J. Mol. Sci.* **18** (2017) 237 (<https://dx.doi.org/10.3390/ijms18030237>)
8. D. N. Rockwood, R. C. Preda, T. Yücel, X. Wang, M. L. Lovett, D. L. Kaplan, *Nat. Protoc.* **6** (2011) 1612 (<https://dx.doi.org/10.1038/nprot.2011.379>)

9. A. Sionkowska, A. Planecka, *Polym. Degrad. Stabil.* **96** (2011) 523 (<https://dx.doi.org/10.1016/j.polymdegradstab.2011.01.001>)
10. S. Krimm, J. Bandekar, *Adv. Protein Chem.* **38** (1986) 181 ([https://dx.doi.org/10.1016/S0065-3233\(08\)60528-8](https://dx.doi.org/10.1016/S0065-3233(08)60528-8))
11. Q. Lu, X. Wang, S. Lu, M. Li, D. L. Kaplan, H. Zhu, *Biomater.* **32** (2011) 1059 (<https://dx.doi.org/10.1016/j.biomaterials.2010.09.072>)
12. R. Nazarov, H. Jin, D. L. Kaplan, *Biomacromolecules* **5** (2004) 718 (<https://dx.doi.org/10.1021/bm034327e>)
13. T. Lefèvre, M. E. Rousseau, M. Pézolet, *Biophys. J.* **92** (2007) 2885 (<https://dx.doi.org/10.1529/biophysj.106.100339>)
14. B. L. Sacco, H. de Santana, *Quím. Nova* **42** (2019) 1014 (<https://dx.doi.org/10.21577/0100-4042.20170413>)
15. M. Preghennella, G. Pezzotti, C. Migliaresi, *J. Raman Spectrosc.* **38** (2007) 522 (<https://dx.doi.org/10.1002/jrs.1675>)
16. M.-E. Rousseau, T. Lefèvre, L. Beaulieu, A. Tetsuo, M. Pézolet, *Biomacromolecules* **5** (2004) 2247 (<https://dx.doi.org/10.1021/bm049717v>)
17. P. Monti, P. Taddei, G. Freddi, T. Asakura, M. Tsukada, *J. Raman Spectrosc.* **32** (2001) 103 (<https://dx.doi.org/10.1002/jrs.675>)
18. P. Monti, G. Freddi, A. Bertoluzza, N. Kasai, M. Tsukada, *J. Raman Spectrosc.* **29** (1998) 297 ([https://dx.doi.org/10.1002/\(SICI\)1097-4555\(199804\)29:4%3C297::AID-JRS240%3E3.0.CO;2-G](https://dx.doi.org/10.1002/(SICI)1097-4555(199804)29:4%3C297::AID-JRS240%3E3.0.CO;2-G))
19. S. D. Aznar-Cervantes, D. Vicente-Cervantes, L. Meseguer-Olmo, J. L. Cenis, A. A. Lozano-Pérez, *Mater. Sci. Eng., C* **33** (2013) 1945 (<https://dx.doi.org/10.1016/j.msec.2013.01.001>)
20. X. Chen, D. P. Knight, Z. Shao, F. Vollrath, *Polym.* **42** (2001) 9969 ([https://dx.doi.org/10.1016/S0032-3861\(01\)00541-9](https://dx.doi.org/10.1016/S0032-3861(01)00541-9))
21. A. Motta, L. Fambri, C. Migliaresi, *Macromol. Chem. Phys.* **203** (2002) 1658 ([https://dx.doi.org/10.1002/1521-3935\(200207\)203:10/11%3C1658::AID-MACP1658%3E3.0.CO;2-3](https://dx.doi.org/10.1002/1521-3935(200207)203:10/11%3C1658::AID-MACP1658%3E3.0.CO;2-3))
22. G. Freddi, G. Pessina, M. Tsukada, *Int. J. Biol. Macromol.* **24** (1999) 251 ([https://dx.doi.org/10.1016/s0141-8130\(98\)00087-7](https://dx.doi.org/10.1016/s0141-8130(98)00087-7)).